Available online at www.sciencedirect.com

ScienceDirect

IFAC PapersOnLine 59-35 (2025) 286–291

Cooperative Trajectory Planning through Negotiation for a Stand-Up Aid

Julian Schneider * Yang Shen * Balint Varga * Sören Hohmann *

* *Institute of Control Systems, Karlsruhe Institute of Technology, Karlsruhe, Germany (e-mail: julian.schneider@kit.edu).*

Abstract: Shared control research offers promising opportunities and improvements for people with limited mobility through robotic assistance, for example in wheelchair applications or rehabilitation systems. Such systems also offer a wide range of possibilities for assisting people with limited mobility out of bed. In contrast to existing works in the field of shared control, in which the reference trajectory is assumed to be known to both partners or is specified by one of them in a leader-follower approach, this work aims to enable both partners to influence the reference trajectory. To this end, two existing approaches from the literature are implemented. The first one is a trajectory deformation approach and the other an existing work on cooperative agreement through trajectory negotiation. Both are investigated in simulations and the results show that the cooperative agreement process requires less control effort on the part of the humans to communicate their trajectory request than in trajectory negotiation. The results thus promise an advantage through cooperation already at the trajectory level of a shared control system.

Keywords: Cooperative trajectory planning, Shared control, Physical human-robot interaction, Human-machine cooperation, Communication.

1. INTRODUCTION

Interactive human–machine systems aim to fuse human strengths with automation in a way that measurably improves task performance while easing cognitive and physical load. This approach aims to create a symbiotic relationship in which human input is seamlessly integrated with automation (Inga et al., 2022). Such systems have been extensively studied and developed under the concept of shared control, in domains such as driver assistance systems (Marcano et al., 2020), robot-assisted minimally invasive surgery (Varga and Poncelet, 2025) and teleoperation technologies (Li et al., 2023; Grobbel et al., 2023). Intelligent wheelchairs represent another prominent application area (Carlson and Demiris, 2012).

Beyond these domains, everyday motions – such as getting elderly and ill people out of bed – pose stringent demands where users face movement restrictions and safety risks, making shared control attractive. In this context, we consider a stand up aid, i.e., a powered assistive device that supports the sit-to-stand transition from bed by providing guided motion and partial weight support for people with limited mobility. Statistics from the German Ministry of Health show just how great the demand is for technical aids, which also include standing aids. In 2023 alone, 11.17 billion Euro was spent on these aids (BMG, 2024). However, many existing systems provide only static, one-size-fits-all support and cannot adapt when a person's preferred movement path differs from the device's default trajectory. A shared control approach would enable individualized support that respects user preferences.

Many shared control methods assume that the cooperative system follows a predefined reference trajectory known to both agents - e.g., the lane center in assisted driving (Claussmann et al., 2020). However, as noted by (Schneider et al., 2024b), this assumption does not universally apply—particularly in contexts such as stand-up assistance systems, where a shared reference trajectory may not exist. Humans and automation each pursue different movement desires. However, different reference trajectories lead to control conflicts (Abbink et al., 2012). Effectively resolving these control conflicts is crucial, as it directly determines whether a stand up aid can provide seamless, individualized support that adapts in real time to the individual preferences and needs of each user.

Two resolving strategies are apparent: (i) a leader–follower scheme in which either the human or the robot prescribes the reference, or (ii) a cooperative scheme in which both agents converge on a common trajectory through negotiation. Since a stand up aid must balance user abilities and needs with device requirements (e.g., ergonomic and safe motion), we pursue the cooperative option.

Such a trajectory cooperation process for finding a common reference trajectory is proposed in (Schneider et al., 2022). It is an emancipated agreement process, i.e., one in which humans and automation are treated equally, with the aim of reaching a consensus on a common trajectory. The application considered in that work is the haptically coupled accompaniment of people with limited mobility by a robot in a hospital.

Peer review under responsibility of International Federation of Automatic Control.
10.1016/j.ifacol.2025.12.490

In this paper, we adapt the same cooperation mechanism to a stand up aid and analyze it in simulation. Using a simulative model, a simulation will show that such a cooperation process with an automation adaptation strategy leads to a lower overall control effort on the part of humans to communicate their trajectory request than an approach from the literature that was examined in comparison. Section 2 presents the related works. Section 3 presents the developed cooperative negotiation algorithm in more detail, as well as the approach from the literature that was considered for comparison. Section 4 shows the simulated comparison of both methods. Section 5 discusses the results.

2. RELATED WORK ON COOPERATIVE TRAJECTORY FINDING

We use the term *cooperation on the trajectory layer* to denote the process by which human and automation jointly determine the reference trajectory in a cooperative system in contrast to adaptive control methods on the action layer, e.g. in (Varga, 2024). Although the term is used heterogeneously and, to the authors' knowledge, lacks a formal definition in the literature, we adopt the perspective of horizontal cooperation within the layer models of human–machine cooperation (HMC) (for HMC-layer models see for example (Abbink et al., 2018; Flemisch et al., 2019; Rothfuß et al., 2019)). The goal of the cooperation on the trajectory layer is to establish a common trajectory when none is implied by the environment or by other contextual information, thereby preventing conflicts that would otherwise surface at the action or execution level. A good summary of this is provided in the paper (Schneider et al., 2024b). It synthesizes cooperative trajectory-planning approaches for shared control and clarifies how human and automation trajectory requests are represented and reconciled. We briefly outline these categories below following (Schneider et al., 2024b).

In *human-dominated methods*, the system explicitly estimates the human's trajectory request (e.g., from control inputs or haptic interaction) and then commands the automation to follow that estimate independently. In some cases, haptic shared control may apply corrective torques/forces to stabilize tracking, but the human retains full control of the reference trajectory (e.g., (Gnatzig et al., 2012; Boink et al., 2014)).

In *automation-dominated methods*, the automation computes a safe or task-optimal trajectory and enforces it, intervening whenever the human deviates beyond admissible limits. Such corrective interventions (e.g., path projection, constraint enforcement) are common in safety-critical driving assistance (Huang et al., 2022; Jiang et al., 2021), where the human's request is secondary or filtered through safety constraints.

There are also strategies where both the human's and the automation's trajectory requests are combined using *weighted fusion approaches*. In these systems, the influence of each agent on the final trajectory is determined by factors such as the human's attention level (Benloucif et al., 2019) or a fixed gain to give the human the opportunity to influence the trajectory of the automation (Losey and O'Malley, 2018). These factors are used to weight the human's trajectory request relative to the automation's. However, challenges with these systems is that either the automation decides the amount of the human's influence (Benloucif et al., 2019) or the human has to continuously communicate his trajectory change request (Losey and O'Malley, 2018).

A more novel and flexible approach is discussed in (Schneider et al., 2022), which introduces a *negotiation-based model* for trajectory planning that allows for equal or emancipated influence on the common reference trajectory with an automation that can adapt to the reference of the human. Here, both the human and the automation continuously contribute to the trajectory planning process through ongoing negotiation. This approach stands in contrast to the traditional leader-follower models, as it allows for an emancipated cooperation, where both agents actively participate in determining the trajectory. This is particularly beneficial in less time- or safety-critical applications, where cooperation and mutual adaptation are more important than rigid control.

While existing methods either prioritize the automation for safety or the human's desires with varying degrees of automation assistance, the negotiation-based approach presents a promising emancipated alternative in which neither humans nor automation are deliberately given ultimate authority. To compare this alternative with an existing approach, the negotiation-based approach from (Schneider et al., 2022) is implemented together with the trajectory deformation approach from (Losey and O'Malley, 2018) and presented in the following section.

3. METHODS FOR COOPERATIVE TRAJECTORY FINDING

3.1 Trajectory deformation

The trajectory deformation approach of (Losey and O'Malley, 2018) is an extension of a classic impedance control approach, in which the robot reacts to a force exerted by a human with a deviation from its original trajectory. With the classic impedance control approach, only the robot's current trajectory can be influenced, but not its future trajectory. The trajectory deformation approach makes it possible to change the future trajectory of the robot within the time interval $\tau = \tau_f - \tau_i$ by applying the force $\boldsymbol{F}_{\mathrm{H}}(\tau_i)$. The idea is that this force causes a deformation of the robot's original trajectory $\gamma_d(t)$ by a vector field $V(t)$. This vector field is described on the one hand by the change in energy caused by the human force $\boldsymbol{F}_{\mathrm{H}}(\tau_i)$. On the other hand, the trajectory should be as similar as possible to a human trajectory by choosing a minimum jerk model. This results in the deformed trajectory $\tilde{\gamma}_d$ from the original trajectory γ_d via the following relationship:

$$\tilde{\gamma}_d = \gamma_d + \mu\delta H F_{\mathrm{H}}(\tau_i). \tag{1}$$

The scalar force component $F_{\mathrm{H}}(\tau)$ corresponds to the force input of the human in the corresponding spatial direction, the parameter μ is a gain factor, δ is the sample time between two waypoints, and H results from energy optimization.

3.2 Trajectory negotiation

The structure of trajectory negotiation follows the system structure proposed in (Schneider et al., 2024a), consisting of a trajectory planning module for the automation, an estimation of the human's desired trajectory from the force $\boldsymbol{F}_{\mathrm{H}}$, a parameter estimation for the human's stubbornness $\boldsymbol{x}_{\mathrm{stubb,H}}$, and an arbitration module, which is implemented as a negotiation module in this work. The trajectory planning of the automation is optimization-based and minimizes both the distance to the origin path $d(\boldsymbol{v}_{\mathrm{A}})$ and the required velocity $\boldsymbol{v}_{\mathrm{A}}$. The parameters w_d and w_v weight the two components. The solution to the optimization $\boldsymbol{v}_{\mathrm{A}}^*$ denotes the optimal desired velocity of the automation on its original trajectory.

$$J_{\mathrm{A}}(\boldsymbol{v}_{\mathrm{A}}) = w_d \cdot d(\boldsymbol{v}_{\mathrm{A}}) + w_v \cdot \boldsymbol{v}_{\mathrm{A}}^T \boldsymbol{v}_{\mathrm{A}} \tag{2}$$

$$\boldsymbol{v}_{\mathrm{A}}^* = \arg\min_{\boldsymbol{v}_{\mathrm{A}}} \{J_{\mathrm{A}}(\boldsymbol{v}_{\mathrm{A}})\} \tag{3}$$

The estimation of the desired trajectory of the automation is based on the estimation of the desired current speed of the human and follows the estimation model from (Schneider et al., 2024a). The components of the estimated desired velocity $\hat{v}_{\mathrm{x}}$, $\hat{v}_{\mathrm{y}}$ and $\hat{v}_{\mathrm{z}}$ of the human (the roof denotes an estimated variable) are derived from an estimated desired acceleration $\Delta\hat{v}_i, i \in x, y, z$ from the measured force $F_{\mathrm{H},i}, i \in \{x, y, z\}$ of the human:

$$\Delta\hat{v}_i = \mathrm{sgn}(F_{\mathrm{H},i}) \frac{\min(|F_{\mathrm{H},i}|, F_{\mathrm{H,max},i})}{F_{\mathrm{H,max},i}} v_{\mathrm{ub}} \cdot f_v \tag{4}$$

The parameter $F_{\mathrm{H,max},i}$ normalizes the human input to a maximum reference value and v_{ub} represent the upper limit for the allowed velocities. The velocity desired by the human is then determined by the velocity currently being executed by the automation and the velocity change desired by the human:

$$\hat{\boldsymbol{v}}_{\mathrm{H}} = \boldsymbol{v}_{\mathrm{A}} + \Delta\hat{\boldsymbol{v}}_{\mathrm{H}}. \tag{5}$$

The main element of the present negotiation approach is the determination of the stubbornness with which a person clings to their desire to move toward their desired original trajectory. The stubbornness model is also taken from (Schneider et al., 2024a) and is supplemented in this work with an additional time-integrating component $\boldsymbol{x}_{\mathrm{stubb,H,I}}$. It reads as follows:

$$x_{\mathrm{stubb,H},i} = x_{\mathrm{stubb,H,I}} + \left|\frac{F_{\mathrm{H},i}}{F_{\mathrm{H,max},i}}\right| \cdot \left|\frac{\max(|\hat{v}_{\mathrm{H},i,k-1} - v_{\mathrm{ub}}|, |\hat{v}_{\mathrm{H},i,k-1} - v_{\mathrm{lb}}|) - |\hat{v}_{\mathrm{H},i,k-1} - v_{\mathrm{A},i,k}|}{\max(|\hat{v}_{\mathrm{H},i,k-1} - v_{\mathrm{ub}}|, |\hat{v}_{\mathrm{H},i,k-1} - v_{\mathrm{lb}}|)}\right| \tag{6}$$

The additional time-integrationg component $\boldsymbol{x}_{\mathrm{stubb,H,I}}$ is calculated via:

$$x_{\mathrm{stubb,H,I},i} = p_{\mathrm{H,I}} \int_0^t |F_{\mathrm{H},i}|\, dt. \tag{7}$$

The second term of Equation (6) comprises two components. The first component accounts for the amplitude of the interaction force and reflects the assumption that a higher amplitude corresponds to greater stubbornness, indicating a stronger adherence to one's own intended motion. The second component represents the extent to which the human's prior motion intention is taken into account. This is achieved by incorporating feedback from the currently executed trajectory - i.e., the unified trajectory at the current time step k - and comparing it with the estimated human motion intention from the previous time step $k-1$. This comparison is expressed through the difference between the human intention $v_{\mathrm{H},i,k-1}$ (reference value) and the actual executed trajectory $v_{\mathrm{A},i,k}$ (measured value). From the human perspective, this mismatch results in a control deviation caused by the influence of the automation's motion intention, which manifests as stubbornness. The first summand in (6) implements the idea that if a person holds on to a force value for a longer period of time, this means greater stubbornness. This corresponds to the temporal integration of the human force scaled with the parameter $p_{\mathrm{H,I}}$, see (7).

Based on the norm of the determined human stubbornness, $\|\boldsymbol{x}_{\mathrm{stubb,H}}\|$ an interaction value I_k is computed at each time step. This value reflects not only the degree of human stubbornness but also its relationship to the behavior of the automation. In the case where the automation behaves fully compliantly ($U_{\mathrm{loss}} = 1$) while the human exhibits maximum stubbornness ($\|\boldsymbol{x}_{\mathrm{stubb,H}}\| = 1$)) the interaction value reaches its maximum possible value of $I_k = 2$. This represents the extreme case in which the human remains fully unyielding despite fully accommodating behavior from the automation:

$$I_k = -2 + 3 \cdot \|\boldsymbol{x}_{\mathrm{stubb,H}}\| + U_{\mathrm{loss}}. \tag{8}$$

An average value is formed over l time steps for smoothing the interaction values:

$$\bar{I} = \frac{1}{l} \cdot \sum_{j=1}^{l} I_j \tag{9}$$

The value of U_{loss} is subsequently derived using configurable parameters $\bar{I}_{\mathrm{min}}$ and $\bar{I}_{\mathrm{max}}$, which allow for the sensitivity of the calculation to be adjusted:

$$U_{\mathrm{loss}} = \frac{\bar{I} - \bar{I}_{\mathrm{min}}}{\bar{I}_{\mathrm{max}} - \bar{I}_{\mathrm{min}}}. \tag{10}$$

The relationship between the utility loss and the remaining utility for the automation, the target utility U_{target}, can be expressed as following:

$$U_{\mathrm{target}} = 1 - U_{\mathrm{loss}}. \tag{11}$$

To achieve the final result, that determines the negotiated result for the automation velocity, an optimisation problem is formulated:

$$\boldsymbol{v}_{\mathrm{A,neg}} = \arg\min_{\boldsymbol{v}} \{(U(\boldsymbol{v}) - U_{\mathrm{target}})^2\}. \tag{12}$$

4. SIMULATION

4.1 Simulation setup

Figure 1 shows a simulated image of the cooperative stand-up aid, which is considered as an example system in this work. A person lying in bed can hold on with his hands to a handle (black) attached to the KUKA end effector, which assists him in getting up by exerting a force. ROS2 is used as the software framework to control the KUKA robot via an Ubuntu PC. The ROS2 framework Moveit2 (Sucan and Chitta, 2025) is used for the inverse kinematics and `iiwa_ros2` (ICube-Robotics, 2025) for controlling the KUKA robot via the FRI interface using joint angles $\boldsymbol{\theta}(t)$. Since the IK-Planner Moveit2-Servo requires Cartesian velocities $\boldsymbol{v}(t)$ as input variables, the reference trajectories from the two approaches to be compared are transferred to Moveit2 as Cartesian velocities.

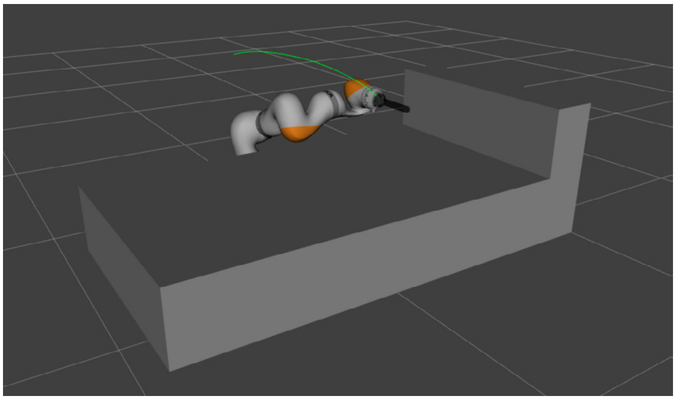

Figure 1. Visualisation of the stand up aid system with the automation reference trajectory (green) in ROS2-Rviz

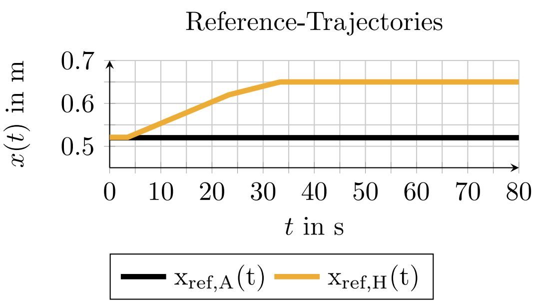

Figure 2. Plot of the reference trajectories for the simulation setup in the x-dimension for the automation (index A) and the human (index H).

Figure 2 shows the reference trajectories in the x-dimension for both the automation and the human. The automation's reference trajectory is constant in the value $x_{\mathrm{ref,A}}(t) = 0.52\,\mathrm{m}$ from the initial position at $t = 0$ to the final position at $t = 80\,\mathrm{s}$. The human's reference increases linearly from $x_{\mathrm{ref,H}}(t = 0\,\mathrm{s}) = 0.52\,\mathrm{m}$ to $x_{\mathrm{ref,H}}(t \approx 33\,\mathrm{s}) = 0.65\,\mathrm{m}$. The human's reference trajectory is thus an offset from the automation's reference trajectory, which leads to a control conflict that must be resolved by the two approaches. The force $F_{\mathrm{H,x}}$ exerted by the human being serves as the communication variable or input for both methods. It is modeled as a simple P-control law and results from the difference $e_x = x_{\mathrm{ref,H}} - x_{\mathrm{current}}$, which is amplified by a constant parameter P_{H}:

$$F_{\mathrm{H,x}} = P_{\mathrm{H}} \cdot e_{\mathrm{x}}. \tag{13}$$

The human is modeled very stubborn during the first 40 s after the start of the movement, meaning that he wants to follow strictly its reference trajectory. Afterwards the human becomes totally compliant, i.e., from this point on, it no longer exerts any force and $F_{\mathrm{H,x}} = 0$ applies. This behavior shall compare the two methods in a phase with a very stubborn human and a compliant human.

The time integral over $F_{\mathrm{H,x}}$ should be considered as a measure of human effort $\mathrm{Eff_H}$ in this simulation:

$$\mathrm{Eff_H} = \int_0^T F_{\mathrm{H,x}}(t)\, dt. \tag{14}$$

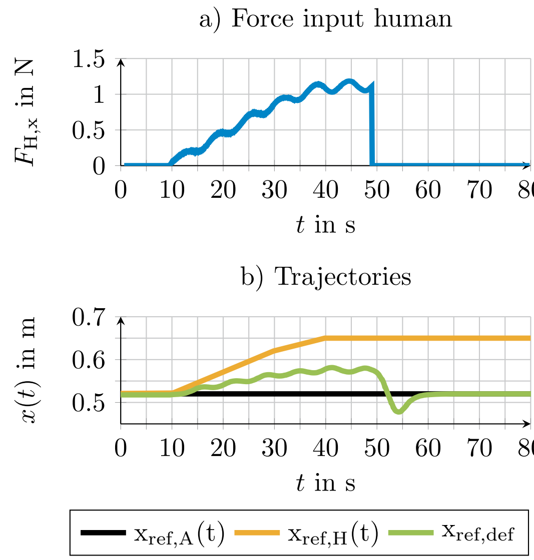

Figure 3. Plot of simulation results for the trajectory deformation approach with $\mu = 0.05$.

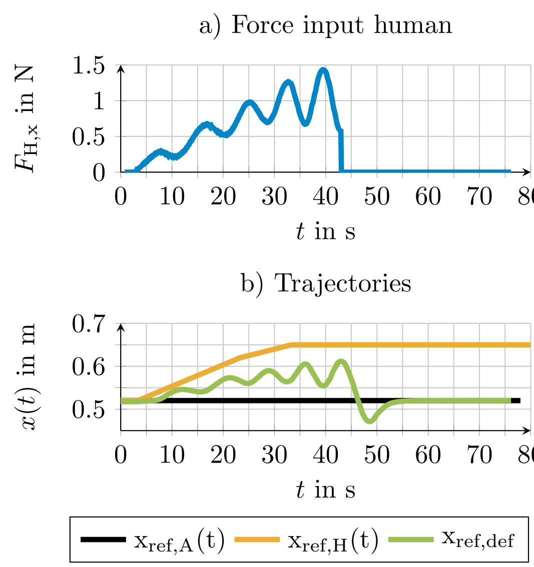

Figure 4. Plot of simulation results for the trajectory deformation approach with $\mu = 0.06$.

4.2 Simulation results

Figures 3 and 4 show the simulation results for trajectory deformation. In Figure 3, the parameter μ was set to 0.05, and in Figure 4 to 0.06. According to (13), a force $F_{\mathrm{H,x}}$ is exerted by the human when $x_{\mathrm{ref,H}}$ and x_{current} differ. After the force is applied, the trajectory in both cases exhibits oscillations. In Figure 3 b), the oscillations are stable, while in Figure 4 c), the oscillation amplitudes increase before the human force drops to 0 N after 40 s. In both simulations, the human force exceeds 1 N, with a peak of nearly 1.5 N in Figure 4. The human effort is $\mathrm{Eff_H} = 28.85\,\mathrm{N\,s}$ for $\mu = 0.05$ and $\mathrm{Eff_H} = 27.18\,\mathrm{N\,s}$ for $\mu = 0.06$. On average, the deformed trajectory approaches only about half the distance to the original reference before the human force drops to 0 N.

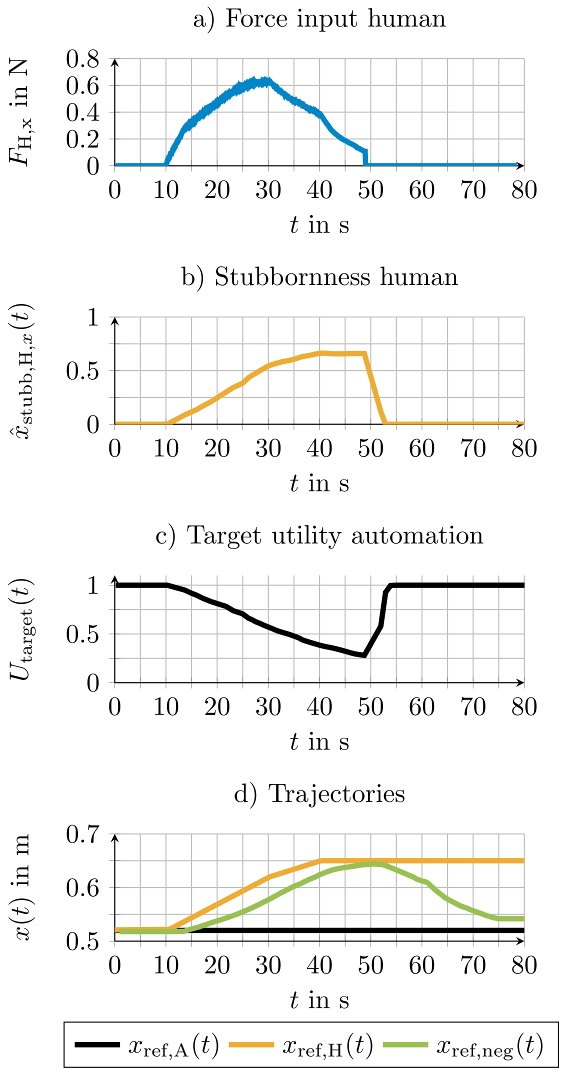

Figure 5. Plot of simulation results for the trajectory negotiation approach.

The results of the trajectory negotiation can be seen in Figure 5. After applying a human force at $t \approx 10\,\mathrm{s}$, the human force rises to a peak of approx. $F_{\mathrm{H,x}} = 0.6\,\mathrm{N}$ before subsequently decreasing again. The stubbornness graph shows that it rises approximately constantly to approx. 0.7 (Figure 5b). The target utility value of the automation decreases as the human's stiffness increases (Figure 5c), causing the automation to deviate further from its desired trajectory (Figure 5d) until the human's desired position is almost reached at $t \approx 50\,\mathrm{s}$. After the human releases the force, the stubbornness drops back to 0, the target utility value of the automation increases, and the negotiated trajectory returns to the desired reference of the automation. The effort required by the human during trajectory negotiation is calculated as $\mathrm{Eff}_{\mathrm{H}} = 15.58\,\mathrm{N\,s}$.

5. DISCUSSION

The simulation results show that trajectory negotiation has advantages over trajectory deformation in three aspects: (1) the negotiated trajectory does not exhibit oscillations, (2) the negotiated trajectory converges toward the $x_{\mathrm{ref,H}}(t)$ in the case of stubborn humans, (3) the trajectory negotiation requires significantly less effort on average for humans to communicate their desired movements.

The results provide promising initial insight and are derived exclusively from simulation and therefore future work must undertake controlled laboratory experiments to validate both approaches and assess their robustness in real use under practical conditions. In particular, the human control law (13) is a modeling assumption; targeted experiments are required to identify the control strategy actually applied by the test subject in this task. Because the oscillatory response during trajectory deformation emerges from this control law, its empirical characterization will be essential for interpreting and refining the observed dynamics.

Finally, it appears that an emancipated approach, in which neither of the two agents has final authority, is well suited for agreeing on a common trajectory. In the case of safety-critical and time-critical applications, however, this is most likely to be different, and final authority is required for one of the two agents.

6. CONCLUSION

In conclusion, the simulation results indicate that the trajectory negotiation approach outperforms trajectory deformation in terms of stability, convergence, and communication efficiency. Future work should focus on validating these findings through real-world experiments and refining the control laws governing human behavior during trajectory negotiation and trajectory deformation.

One main challenge across all the methods, however, remains ensuring that the fusion of the human's and automation's requests does not lead to unsafe outcomes.

ACKNOWLEDGEMENTS

This work was supported by the German Federal Ministry for Economic Affairs and Climate Action (BMWK) under the grant no. KK5574201AJ3.

REFERENCES

Abbink, D.A., Carlson, T., Mulder, M., de Winter, J.C.F., Aminravan, F., Gibo, T.L., and Boer, E.R. (2018). A Topology of Shared Control Systems—Finding Common Ground in Diversity. *IEEE Transactions on Human-Machine Systems*, 48(5), 509–525.

Abbink, D.A., Mulder, M., and Boer, E.R. (2012). Haptic shared control: Smoothly shifting control authority? *Cognition, Technology & Work*, 14(1), 19–28.

Benloucif, A., Nguyen, A.T., Sentouh, C., and Popieul, J.C. (2019). Cooperative Trajectory Planning for Haptic Shared Control Between Driver and Automation in Highway Driving. *IEEE Transactions on Industrial Electronics*, 66(12), 9846–9857.

BMG, . (2024). Ausgaben für heil- und hilfsmittel der gesetzlichen krankenversicherung (gkv) in deutschland von 2006 bis 2023 (in milliarden euro) [graph]. `https://de.statista.com/statistik/daten/studie/247274/umfrage/ausgaben-fuer-heil-und-hilfsmittel-der-gkv/`. Accessed: 2024-08-29.

Boink, R., van Paassen, M.M., Mulder, M., and Abbink, D.A. (2014). Understanding and reducing conflicts between driver and haptic shared control. In *2014 IEEE International Conference on Systems, Man, and Cybernetics (SMC)*, 1510–1515.

Carlson, T. and Demiris, Y. (2012). Collaborative Control for a Robotic Wheelchair: Evaluation of Performance, Attention, and Workload. *IEEE Transactions on Systems, Man, and Cybernetics, Part B (Cybernetics)*, 42(3), 876–888.

Claussmann, L., Revilloud, M., Gruyer, D., and Glaser, S. (2020). A Review of Motion Planning for Highway Autonomous Driving. *IEEE Transactions on Intelligent Transportation Systems*, 21(5), 1826–1848.

Flemisch, F., Abbink, D.A., Itoh, M., Pacaux-Lemoine, M.P., and Weßel, G. (2019). Joining the blunt and the pointy end of the spear: Towards a common framework of joint action, human–machine cooperation, cooperative guidance and control, shared, traded and supervisory control. *Cognition, Technology & Work*, 4(21), 555–568.

Gnatzig, S., Schuller, F., and Lienkamp, M. (2012). Human-machine interaction as key technology for driverless driving - A trajectory-based shared autonomy control approach. In *2012 IEEE RO-MAN: The 21st IEEE International Symposium on Robot and Human Interactive Communication*, 913–918.

Grobbel, M., Varga, B., and Hohmann, S. (2023). Shared Telemanipulation with VR Controllers in an Anti Slosh Scenario. In *2023 IEEE International Conference on Systems, Man, and Cybernetics (SMC)*, 4405–4410.

Huang, C., Huang, H., Zhang, J., Hang, P., Hu, Z., and Lv, C. (2022). Human-Machine Cooperative Trajectory Planning and Tracking for Safe Automated Driving. *IEEE Transactions on Intelligent Transportation Systems*, 23(8), 12050–12063.

ICube-Robotics (2025). IIWA_ROS2. https://github.com/ICube-Robotics/iiwa_ros2.

Inga, J., Ruess, M., Heinrich Robens, J., Nelius, T., Rothfuß, S., Kille, S., Dahlinger, P., Lindenmann, A., Thomaschke, R., Neumann, G., Matthiesen, S., Hohmann, S., and Kiesel, A. (2022). Human-Machine Symbiosis: A Multivariate Perspective for Physically Coupled Human-Machine Systems. *International Journal of Human-Computer Studies*, 170, 102926.

Jiang, B., Li, X., Zeng, Y., and Liu, D. (2021). Human-Machine Cooperative Trajectory Planning for Semi-Autonomous Driving Based on the Understanding of Behavioral Semantics. *Electronics*, 10(8), 946.

Li, G., Li, Q., Yang, C., Su, Y., Yuan, Z., and Wu, X. (2023). The Classification and New Trends of Shared Control Strategies in Telerobotic Systems: A Survey. *IEEE Transactions on Haptics*, 16(2), 118–133.

Losey, D.P. and O'Malley, M.K. (2018). Trajectory Deformations From Physical Human–Robot Interaction. *IEEE Transactions on Robotics*, 34(1), 126–138.

Marcano, M., Díaz, S., Pérez, J., and Irigoyen, E. (2020). A Review of Shared Control for Automated Vehicles: Theory and Applications. *IEEE Transactions on Human-Machine Systems*, 50(6), 475–491.

Rothfuß, S., Schmidt, R., Flad, M., and Hohmann, S. (2019). A Concept for Human-Machine Negotiation in Advanced Driving Assistance Systems. In *2019 IEEE International Conference on Systems, Man and Cybernetics (SMC)*, 3116–3123.

Schneider, J., Rothfuß, S., and Hohmann, S. (2022). Negotiation-based cooperative planning of local trajectories. *Frontiers in Control Engineering*, 3.

Schneider, J., Straky, N., Meyer, S., Varga, B., and Hohmann, S. (2024a). Reacting on Human Stubbornness in Human-Machine Trajectory Planning. In *2024 IEEE International Conference on Systems, Man, and Cybernetics (SMC)*, 909–915.

Schneider, J., Varga, B., and Hohmann, S. (2024b). Cooperative trajectory planning: Principles for human-machine system design on trajectory level. *at - Automatisierungstechnik*, 72(12), 1121–1129.

Sucan, I.A. and Chitta, S. (2025). MoveIt. moveit.ros.org.

Varga, B. (2024). Toward adaptive cooperation: Model-based shared control using lq-differential games. *Acta Polytechnica Hungarica 2024*, 21(10), 439 – 456.

Varga, B. and Poncelet, M. (2025). A shared control approach to the robot-assisted cataract surgery training for novice surgeons. *Sensors*. In press.